Evolution, 60(1), 2006, pp. 24–30

PARASITE LOCAL ADAPTATION IN A GEOGRAPHIC MOSAIC

SCOTT L. NUISMER
Department of Biological Sciences, University of Idaho, Moscow, Idaho 83844
E-mail: snuismer@uidaho.edu

Abstract.—A central prediction of the geographic mosaic theory of coevolution is that coevolving interspecific interactions will show varying degrees of local maladaptation. According to the theory, much of this local maladaptation is driven by selection mosaics and spatially intermingled coevolutionary hot and cold spots, rather than a simple balance between gene flow and selection. Here I develop a genetic model of host-parasite coevolution that is sufficiently general to incorporate selection mosaics, coevolutionary hot and cold spots, and a diverse array of genetic systems of infection/resistance. Results from this model show that the selection mosaics experienced by the interacting species are an important determinant of the sign and magnitude of local maladaptation. In some cases, this effect may be stronger than a previously described effect of relative rates of parasite and host gene flow. These results provide the first theoretical evidence that selection mosaics and coevolutionary hot and cold spots per se determine the magnitude and sign of local maladaptation. At the same time, however, these results demonstrate that coevolution in a geographic mosaic can lead to virtually any pattern of local adaptation or local maladaptation. Consequently, empirical studies that describe only patterns of local adaptation or maladaptation do not provide evidence either for or against the theory.

Key words.—Gene flow, host, local maladaptation, parasite, population structure, selection mosaic.

Received July 14, 2005. Accepted October 20, 2005.

The geographic mosaic theory predicts that local maladaptation is a common and defining characteristic of coevolving species interactions (Thompson 1994, 1999, 2005). The extent to which these patterns emerge from the unique components of the geographic mosaic theory (selection mosaics and intermingled coevolutionary hot and cold spots) rather than simply a balance between selection and gene flow (e.g., Fisher 1950; Endler 1973; Slatkin 1973) is largely unclear. Previous models have shed little light on this issue for several reasons. First, many coevolutionary models have not explicitly considered selection mosaics or coevolutionary hot spots and, thus they cannot support or refute the key predictions of the geographic mosaic theory. Second, models that have explicitly incorporated these essential components of the theory have often been based upon haploid genetics and have generally considered only a single type of genetic interaction between species (Nuismer et al. 1999, 2000; Gomulkiewicz et al. 2000).

Here I develop and analyze a simple model of spatially structured host-parasite coevolution that incorporates diploid organisms and is sufficiently general to incorporate both selection mosaics and coevolutionary hot spots, as well as a diverse array of empirically motivated genetic systems of infection and resistance. A specific goal is to elucidate how selection mosaics resulting from spatial variation in the fitness consequences of infection and resistance shape emerging patterns of local adaptation.

MODEL DESCRIPTION

I consider coevolution between a host and parasite that is mediated by a single diploid locus with two alleles in each species, A and a in the host and B and b in the parasite. Each species occupies a landscape characterized by two discrete habitat patches connected by host and parasite movement at rates m_H and m_P, respectively. The frequency of the A allele in host population i is denoted $p_{A,i}$ and the frequency of the B allele in parasite population i is denoted $p_{B,i}$. Both species are assumed to mate at random, undergo symmetric mutation at rates μ_H and μ_P and have population sizes sufficiently large for the effects of genetic drift to be ignored.

Interactions between species are assumed to be governed by one of the following empirically motivated genetic systems of infection and resistance. The gene-for-gene model (hereafter GFG) has been demonstrated to be widespread in plant-pathogen interactions and is characterized by resistance alleles in the host (generally dominant) that confer resistance to parasite avirulence genes (generally dominant; Flor 1956; Thompson and Burdon 1992). Several recent studies have documented costs associated with host resistance alleles and parasite virulence alleles (Thrall and Burdon 2003; Tian et al. 2003); therefore, such costs are included in the model. The matching alleles model (hereafter MA) is predicated upon a system of self-nonself recognition and assumes that hosts can only successfully mount an immune response against parasites that carry alleles that can be recognized as nonself (Peters and Lively 1999; Agrawal and Lively 2002). The inverse matching alleles model (hereafter IMA) assumes that hosts can mount a successful immune response against only those parasites carrying alleles that can be matched by the hosts arsenal of recognition alleles as is the case for the vertebrate major histocompatibility complex (MHC) system (Frank 2002). For each genetic system of infection/resistance, successful infection is assumed to reduce host fitness by an amount s_H, whereas unsuccessful infection is assumed to reduce parasite fitness by an amount s_P (Fig. 1). Thus, the quantities s_H and s_P measure the ecological consequences of interspecific interactions (e.g., virulence) and are assumed independent of host and parasite genotypes. From this point forward, these quantities will be termed ''interaction coefficients.''

The life cycle of both species is assumed to begin with selection, after which the frequencies of host and parasite alleles are given by:

Parasite Genotype \ Host Genotype	AA	Aa	aa
BB	{I,R,I}	{I,R,I}	{R,I,I}
Bb	{R,R,R}	{I,R,R}	{R,R,I}
bb	{R,I,R}	{I,R,R}	{I,R,I}

FIG. 1. The outcome (I, infect, R, resist) of encounters between parasite and host genotypes for the various genetic models of infection/resistance. Each vector represents the outcome of the interaction for the matching alleles model, inverse matching alleles model, and gene-for-gene model, respectively. If an infection occurs (I entries) host fitness is reduced by s_H, whereas if resistance occurs (R entries) parasite fitness is reduced by s_P.

$$p'_{A,i} = \frac{W_{AA,i}p^2_{A,i} + W_{Aa,i}p_{A,i}q_{A,i}}{\bar{W}_{H,i}} \quad \text{and} \tag{1a}$$

$$p'_{B,i} = \frac{W_{BB,i}p^2_{B,i} + W_{Bb,i}p_{B,i}q_{B,i}}{W_{P,i}}, \tag{1b}$$

where $q_{A,i}$ and $q_{B,i}$ are the frequencies of the a and b alleles in population i, respectively. The genotypic fitnesses used in these recursions are:

$$W_{AA,i} = [p^2_{B,i}(1 - \xi_{H,i} - \gamma_{H,i}) + 2p_{B,i}q_{B,i} + q^2_{B,i}(1 - \alpha_{H,i})](1 - \tau_H), \tag{2a}$$

$$W_{Aa,i} = [p^2_{B,i}(1 - \xi_{H,i} - \gamma_{H,i}) + 2p_{B,i}q_{B,i}(1 - \xi_{H,i}) + q^2_{B,i}(1 - \xi_{H,i})](1 - \tau_H), \tag{2b}$$

$$W_{aa,i} = p^2_{B,i}(1 - \alpha_{H,i} - \gamma_{H,i}) + 2p_{B,i}q_{B,i}(1 - \gamma_{H,i}) + q^2_{B,i}(1 - \xi_{H,i} - \gamma_{H,i}), \tag{2c}$$

$$W_{BB,i} = [p^2_{A,i}(1 - \alpha_{P,i}) + 2p_{A,i}q_{A,i}(1 - \alpha_{P,i}) + q^2_{A,i}(1 - \xi_{P,i})](1 - \tau_P), \tag{2d}$$

$$W_{Bb,i} = p^2_{A,i}(1 - \alpha_{P,i} - \xi_{P,i} - \gamma_{P,i}) + 2p_{A,i}q_{A,i}(1 - \alpha_{P,i} - \gamma_{P,i}) + q^2_{A,i}(1 - \alpha_{P,i} - \xi_{P,i}), \quad \text{and} \tag{2e}$$

$$W_{bb,i} = p^2_{A,i}(1 - \xi_{P,i} - \gamma_{P,i}) + 2p_{A,i}q_{A,i}(1 - \alpha_{P,i} - \gamma_{P,i}) + q^2_{A,i}(1 - \alpha_{P,i}), \tag{2f}$$

where i is an index of population and $\xi_{X,i}$ is the interaction coefficient ($s_{X,i}$) for species X due to matching alleles interactions, $\alpha_{X,i}$ is the interaction coefficient ($s_{X,i}$) for species X due to inverse matching alleles interactions, $\gamma_{X,i}$ is the interaction coefficient ($s_{X,i}$) for species X due to gene-for-gene interactions, and τ_X is the spatially homogenous fitness cost of carrying resistance or virulence alleles for species X in the gene-for-gene model. The population mean fitness of host and parasite in patch i is defined in the standard way as:

$$\bar{W}_{H,i} = p^2_{A,i}W_{AA,i} + 2p_{A,i}q_{A,i}W_{Aa,i} + q^2_{A,i}W_{aa,i} \quad \text{and} \tag{3a}$$

$$\bar{W}_{P,i} = p^2_{B,i}W_{BB,i} + 2p_{B,i}q_{B,i}W_{Bb,i} + q^2_{B,i}W_{bb,i}. \tag{3b}$$

Following selection, both species move between populations:

$$p''_{A,i} = p'_{A,i}(1 - m_H) + p'_{A,j}m_H \quad \text{and} \tag{4a}$$

$$p''_{B,i} = p'_{B,i}(1 - m_P) + p'_{B,j}m_P, \tag{4b}$$

where i and j represent the two populations. The last step in the life cycle is mutation:

$$p'''_{A,i} = p''_{A,i}(1 - \mu_H) + (1 - p''_{A,i})\mu_H \quad \text{and} \tag{5a}$$

$$p'''_{B,i} = p''_{B,i}(1 - \mu_P) + (1 - p''_{B,i})\mu_P, \tag{5b}$$

where i is again an index of population identity.

Although it is straightforward to follow changes in the allele frequencies $p_{A,i}$ and $p_{B,i}$ over the course of coevolution, a change of variables and parameters simplifies intuition and facilitates a key approximation. Specifically, I introduce the new variables $\bar{p}_Y = (p_{Y,1} + p_{Y,2})/2$ and $\delta_Y = p_{Y,1} - p_{Y,2}$ which describe the spatial average frequency of allele Y and the spatial difference in the frequency of allele Y across the two patches, respectively. Thus, if δ_Y equals zero there is no spatial genetic structuring. Similarly, I introduce the new parameters $\bar{s}_X = (s_{X,1} + s_{X,2})/2$ and $\delta_{S,X} = s_{X,1} - s_{X,2}$ which describe the spatial average of interaction coefficients for species X and the spatial difference in interaction coefficients for species X, respectively. In terms of the new parameters, selection mosaics and coevolutionary hot or cold spots have particularly simple mathematical representations: anytime $\delta_{S,X}$ does not equal zero for both species, a selection mosaic or intermingled hot and cold spot exists (note that intermingled hot and cold spots are simply extreme selection mosaics where at least one $s_{X,i} = 0$). These definitions are consistent with previous theory (Nuismer et al. 1999, 2000, 2003; Gomulkiewicz et al. 2000; Thompson et al. 2002; Thompson 2005). In addition to simplifying the mathematical definitions of selection mosaics, this change of variables allows the development of an important approximation.

ANALYTICAL RESULTS

If interaction coefficients are weak in an absolute sense ($s_{X,i} \ll 1$) and relative to the rate of gene flow ($s_{X,i} \ll m_X$), a quasi-equilibrium state should be reached where the differences in allele frequencies across the two populations, δ_Y, are small and rapidly changing relative to the average allele frequencies, $\bar{p}_Y$ (see Appendix available online only at http://dx.doi.org/10.1554/05-380.1.s1). Under these conditions, the spatial differences in allele frequency approach the following values:

$$\hat{\delta}_A = \frac{\delta_{S,H}(1 - 2m_H)\bar{p}_A\bar{q}_A}{2m_H}(\kappa_{H,j}) \quad \text{and} \tag{6a}$$

$$\hat{\delta}_B = -\frac{\delta_{S,P}(1 - 2m_P)\bar{p}_B\bar{q}_B}{2m_P}(\kappa_{P,j}), \tag{6b}$$

where, $\kappa_{i,j}$ measures the effect of species interactions of genetic form j (e.g., GFG, IMA, MA) on species i (see online

Appendix). The assumptions of weak interaction coefficients and substantial gene flow used to derive equations (6a,b) will later be relaxed with numerical simulations.

Equations (6a,b) reveal two important results. First, if a species does not experience a selection mosaic ($\delta_{S,X} = 0$), it will not exhibit spatial genetic structure regardless of the average allele frequencies $\bar{p}_A$ and $\bar{p}_B$. Thus, a selection mosaic is required for spatial structuring of allele frequencies to be maintained indefinitely. Second, the quasi-equilibrium amount of spatial genetic structure that can be maintained increases with the strength of the selection mosaic but decreases with increasing rates of gene flow. Neither result assumes that average allele frequencies $\bar{p}_A$ and $\bar{p}_B$ are at equilibrium nor does either result depend upon the rates of mutation in the interacting species.

If local adaptation is defined in the conventional way (Gandon et al. 1996; Kaltz and Shykoff 1998; Dybdahl and Storfer 2003), equations (6a,b) can be used to predict the sign and magnitude of local adaptation at any point in time. Specifically, species i is defined to be locally adapted if an encounter between a randomly selected individual of species i and a randomly selected individual of species j yields a higher expected fitness when the two individuals are drawn from the same (vs. different) populations. Although other definitions of local adaptation are possible (Thompson et al. 2002; Kawecki and Ebert 2004), the conventional definition is used because it facilitates comparison with previous theoretical and empirical results. Using this definition in conjunction with equations (6a,b) (see online Appendix) leads to general solutions for local adaptation in the interacting species:

$$\hat{\theta}_H = -\frac{s_{H,T}\delta_{S,H}\delta_{S,P}\bar{p}_A\bar{q}_A\bar{p}_B\bar{q}_B(1 - 2m_H)(1 - 2m_P)}{2m_H m_P}\pi_i \quad (7a)$$

and

$$\hat{\theta}_P = \frac{s_{P,T}\delta_{S,H}\delta_{S,P}\bar{p}_A\bar{q}_A\bar{p}_B\bar{q}_B(1 - 2m_H)(1 - 2m_P)}{2m_H m_P}\pi_i, \quad (7b)$$

where, π_i measures the effect of species interactions of genetic form i (e.g., GFG, IMA, MA), and $s_{H,T}$ and $s_{P,T}$ are the interaction coefficients acting on the host and parasite, respectively, in a common testing environment. In all cases, the symmetry of the model ensures that if the parasite is locally adapted the host will be locally maladapted and vice versa.

Equations (7a,b) reveal three previously unreported properties of local adaptation in coevolving host-parasite interactions. First, both species must experience a selection mosaic for local adaptation to be permanent. Second, the magnitude of local adaptation increases with the magnitude of the product of the selection mosaics, but decreases with increasing rates of gene flow. Third, for any set of average allele frequencies (which are included in the π terms) the product of the selection mosaics determines which species is locally adapted. This last result, in combination with the information contained in the π terms, can be used to predict which species is expected to be locally adapted over the entire time course of coevolution (see online Appendix). These predictions are summarized in Table 1 and show that parasite local adaptation is favored by congruent selection mosaics ($\delta_{s,H}\delta_{s,P} > 0$) in the MA and GFG models but by incongruous selection mosaics ($\delta_{s,H}\delta_{s,P} < 0$) in the IMA model. Because of model symmetry, the conditions that favor host local adaptation are exactly reversed.

TABLE 1. Conditions for parasite local adaptation.

Model	Parasite locally adapted
Matching alleles	$\delta_{S,H}\delta_{S,P} > 0$*
Inverse matching alleles	$\delta_{S,H}\delta_{S,P} < 0$*
Gene-for-gene	$\delta_{S,H}\delta_{S,P} > 0$

* Results for the matching alleles and inverse matching alleles models assume that average allele frequencies do not concentrate in several regions (details in Appendix available online only at http://dx.doi.org/05-380.1.s1).

The central importance of selection mosaics in shaping patterns of local adaptation follows from the structure of genetic interactions in the various coevolutionary models. The appendix shows that congruent selection mosaics generally lead to spatially congruent allele frequencies in parasite and host for both the IMA and MA models. With this established, it is clear that congruent selection mosaics favor parasite local adaptation in the MA model because parasites must match host allele frequencies to infect. Similarly, it is clear that congruent selection mosaics favor parasite local maladaptation in the IMA model because parasites must mismatch host allele frequencies to infect. The intuition underlying the gene-for-gene model is somewhat more complex and requires an explicit consideration of dominance. When selection mosaics are congruent in the GFG model, so, too, are the spatial differences in allele frequencies (see online Appendix). As a consequence, one habitat patch has a somewhat greater frequency of both virulence and resistance alleles than the other. Individual hosts from the high-resistance patch will, on average, perform substantially better when challenged by foreign parasites drawn from the low-virulence patch. In contrast, individual hosts drawn from the low-resistance patch will do only slightly worse when challenged by foreign parasites drawn from the high-virulence patch due to the patterns of dominance generally observed in GFG interactions (virulence alleles are generally recessive, whereas resistance alleles are generally dominant). Consequently, hosts will be locally maladapted on average. The same logic works in reverse for the case of incongruent selection mosaics.

SIMULATION RESULTS

To evaluate whether results presented in Table 1 are robust when the assumptions of weak interaction coefficients and substantial gene flow are violated, numerical simulations were used to directly iterate the exact recursions over a broad range of parameter combinations. Each simulation calculated the average value of local adaptation for each species over 5000 generations. Runs with an average value of local adaptation below 1×10^{-5} were considered to show no local adaptation; increasing this threshold to 1×10^{-3} had no qualitative impact on the results. For each genetic model of interaction, simulations were run for all possible combinations of the following average interaction coefficients (1/64, 1/32, 1/16, 1/8, 1/4), selection mosaics ($-2\bar{s}$, $-[4/3]\bar{s}$, $-[2/3]\bar{s}$, 0, $[2/3]\bar{s}$, $[4/3]\bar{s}$, $2\bar{s}$), and rates of gene flow (1/256, 1/128, 1/64, 1/32, 1/16, 1/8). For each set of parameters, 10

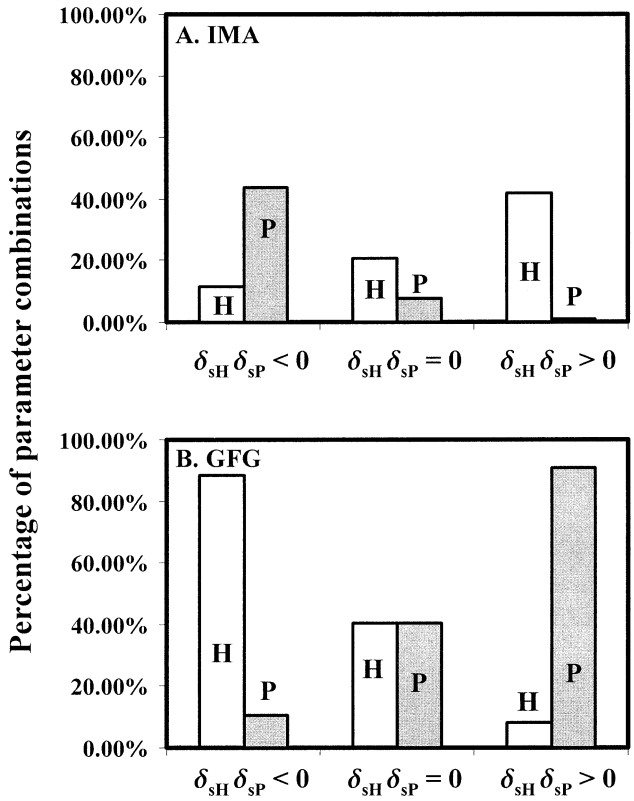

FIG. 2. The percentage of parameter combinations causing local adaptation to evolve in the host (white) and parasite (gray) for cases in which selection mosaics are incongruent ($\delta_{SH}\delta_{SP} < 0$), one or both species lack a selection mosaic ($\delta_{SH}\delta_{SP} = 0$), or selection mosaics are congruent ($\delta_{SH}\delta_{SP} > 0$). (A) Values for the inverse matching alleles model; (B) values for the gene-for-gene model. Because the matching alleles model fails to generate local adaptation of any sort in 99.18% of cases, a similar panel for this model is not shown.

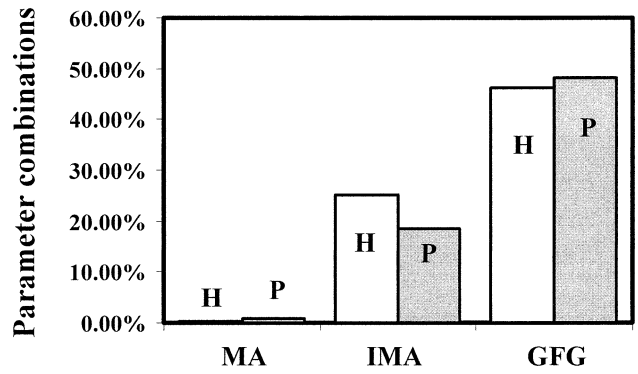

FIG. 3. The total percentage of parameter combinations causing local adaptation to evolve in the host (white) and parasite (gray) for the matching alleles (MA), inverse matching alleles (IMA), and the gene-for-gene (GFG) models. Results based upon simulations of the exact recursions for the 44,100 parameter combinations described in the text.

replicates were run with randomly selected initial allele frequencies, and, for the GFG model, randomly selected (and spatially homogenous) costs of resistance and virulence ranging from 0% to 75% of the average strength of selection. Local adaptation was calculated for each set of parameters as the average value observed across the 10 replicates. In total, 441,000 simulations were run for 44,100 different parameter combinations. The majority of these parameter combinations violate the assumptions of the analytical model.

Simulation results demonstrate that for the GFG and IMA models, the analytical results shown in Table 1 predict the identity of the locally adapted species quite accurately (Fig. 2). For instance, the analytical results predict that in the GFG model the parasite should be locally adapted anytime the selection mosaics of the two species are congruent ($\delta_{S,H}\delta_{S,P} > 0$). Simulation results show that this prediction is borne out: with congruent selection mosaics the parasite is 11.23 times more likely to be locally adapted than the host (Fig. 2). Similar levels of agreement are seen for the IMA model. For instance, analytical results predict the parasite will be locally adapted anytime the selection mosaics of the two species are incongruent ($\delta_{S,H}\delta_{S,P} < 0$). Simulation results support this prediction, demonstrating that with incongruent selection mosaics the parasite is 3.81 times more likely to be locally adapted than the host (Fig. 2).

Although simulation results provide broad support for the importance of selection mosaics in determining patterns of local adaptation in the GFG and IMA models, this is not the case for the MA model. The surprising reason for this discrepancy is that the MA model offers little scope for the evolution of local adaptation of any sort. In fact, simulation results show that the MA model leads to the evolution of local adaptation in either species in only 1.00% of cases (Fig. 3). This result arises because the MA model fails to produce persistent allele frequency cycles. Instead, both host and parasite generally approach fixation for the same set of matching alleles in both populations. The reason is that the diploid MA model generates effective underdominance in the host, preventing host escape from the parasite. In contrast, simulations show that the IMA and GFG models readily produce local adaptation with 43.6% of IMA simulations and 94.3% of GFG simulations leading to local adaptation of either host or parasite (Fig. 3). Thus, as long as costs of resistance and virulence are present, the GFG model generates the highest percentage of cases in which local adaptation occurs.

In addition to calculating the percentage of parameter combinations that lead to local adaptation, simulations were used to quantify the mean and standard deviation of the magnitude of local adaptation for each genetic model of interaction (Fig. 4). The results show that those genetic models of interaction that produce local adaptation most frequently (GFG and IMA) also produce the greatest magnitudes of local adaptation (cf. Figs. 3 and 4). It is important to note, however, that the average magnitude of local adaptation produced by all of the genetic models is quite small.

Previous theoretical studies demonstrated that the relative rates of gene flow in host and parasite can play an important role in determining which species is locally adapted (Gandon et al. 1996; Gandon 1998, 2002; Lively 1999). Analytical results reported here, however, provide no support for this prediction (see eqs. 7a,b). To evaluate whether this discrepancy is simply a consequence of the weak selection and substantial gene flow assumed by the analytical model, I tested

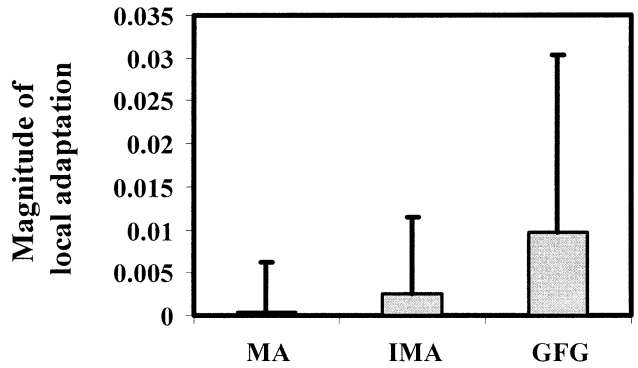

FIG. 4. The average magnitude and standard deviation of local adaptation for the matching alleles (MA), inverse matching alleles (IMA), and the gene-for-gene (GFG) models. Results based upon simulations of the exact recursions for the 44,100 parameter combinations described in the text.

for this effect using data from the numerical simulations (Fig. 5). Thus, simulations considered all possible combinations of host and parasite gene flow from the following range: (1/256, 1/128, 1/64, 1/32, 1/16, 1/8). These simulations reveal that relative rates of gene flow do indeed have an impact on the identity of the locally adapted species, although this effect is quite modest when compared to the selection mosaic effect (cf. Figs. 2 and 5).

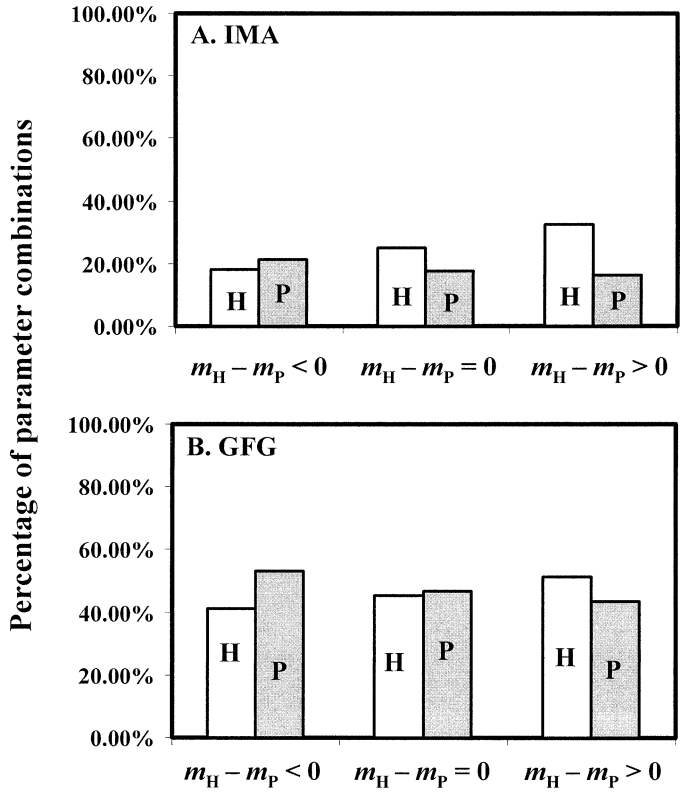

FIG. 5. The percentage of parameter combinations causing local adaptation to evolve in the host (white) and parasite (gray) for cases in which the rate of parasite gene flow exceeds the rate of host gene flow ($m_H - m_P < 0$), the rate of parasite gene flow equals the rate of host gene flow ($m_H - m_P = 0$), or the rate of parasite gene flow is less than the rate of host gene flow ($m_H - m_P > 0$). (A) Values for the inverse matching alleles model, (B) values for the gene-for-gene model. Because the matching alleles model fails to generate local adaptation of any sort in 99.18% of cases, a similar panel for this model is not shown.

DISCUSSION

I have used a simple yet biologically plausible model to demonstrate for the first time that two unique components of the geographic mosaic theory of coevolution—selection mosaics and spatially intermingled coevolutionary hot and cold spots—are critical determinants of the magnitude and sign of local adaptation. This result is not simply a consequence of the balance between gene flow and local selection that generates local adaptation in classical single-species models (Haldane 1948; Endler 1973; Slatkin 1973) and can, in principle, be tested in some natural systems (Lively 1999; Kraaijeveld and Godfray 2001; Thompson and Cunningham 2002).

In addition to providing theoretical support for a key prediction of the geographic mosaic theory, results presented here document important and previously unreported consequences of ploidy. Specifically, analysis of the diploid model considered here demonstrates that the matching alleles model does not lead to persistent cycles and, hence, does not allow persistent patterns of local maladaptation. The absence of persistent cycles in the MA model is a direct consequence of the underdominance inherent to diploid matching alleles models and was not observed in previous models because both host and parasite were assumed to be haploid (Gandon et al. 1996; Lively 1999; Nuismer et al. 2000; Gandon 2002). This result further illustrates the importance of ploidy for coevolutionary dynamics (Switkes and Moody 2001; Lively et al. 2004; Nuismer and Otto 2004).

Results presented here also provide new insight into the causes of local adaptation in host-parasite interactions. Previous population genetic studies have demonstrated that relative rates of gene flow in host and parasite influence the sign and magnitude of local maladaptation (Gandon et al. 1996; Gandon 1998, 2002). Results presented here support this result, but show that the contribution of differences in rates of gene flow across species can be quite weak. Often, the specific structure of selection mosaics is the dominant determinant of the sign and magnitude of local maladaptation. This result has implications for the interpretation of empirical data demonstrating local adaptation of parasites in some systems but local maladaptation of parasites in others (Ballabeni and Ward 1993; Morand et al. 1996; Kaltz et al. 1999; Thrall et al. 2002). Specifically, results presented here show that this pattern may be just as likely due to variation in the structure of selection mosaics across systems as to differences in rates of parasite and host gene flow as is commonly assumed (Kaltz et al. 1999; Gandon 2002; Lively et al. 2004).

Teasing apart the relative contributions of selection mosaics and differences in rates of gene flow will be an important challenge for future theoretical and empirical studies. From a theoretical perspective, it will be necessary to define conditions under which each effect is likely to be most important. Previous studies have shown, for instance, that the effect of relative rates of parasite and host gene flow is most important when overall rates of gene flow are quite low (Gandon et al. 1996; Gandon 1998, 2002). Thus, low rates of gene flow in

both host and parasite may reduce the relative importance of the selection mosaic effect. Other potentially important factors include population sizes, mutation rates, and the genetic basis of infection and resistance. From an empirical perspective, it will be necessary to evaluate the congruence of selection mosaics, relative rates of gene flow, and patterns of local adaptation simultaneously. Although techniques for estimating rates of gene flow and patterns of local adaptation are well established (Lively and Dybdahl 2000; Beerli and Felsenstein 2001; Nielsen and Wakeley 2001; Gandon 2002; Dybdahl and Storfer 2003; Hey and Nielsen 2004), no practical methodology exists for determining the congruence of selection mosaics. In the following paragraph, I provide a conceptual illustration of how the spatial congruence of selection mosaics could be evaluated. I then point to several pitfalls that can arise even in this highly idealized case.

Selection mosaics are defined here and elsewhere (Nuismer et al. 2000; Thompson 2005) as cases in which at least one interaction coefficient ($s_{X,i}$) is spatially variable. Such scenarios arise readily when the ecological consequences of an interaction vary over space (Thompson 1994, 2005). For instance, if parasite infection decreases host fitness more in environment 1 than in environment 2, the interaction coefficient for the host ($s_{H,i}$) is likely to be greater in environment 1 than in environment 2, and therefore $\delta_{S,H} > 0$. Similarly, if a failure to infect a host decreases parasite fitness more in environment 1 than in environment 2, the interaction coefficient for the parasite ($s_{P,i}$) is likely to be greater in environment 1 than in environment 2, and therefore $\delta_{S,P} > 0$. Under this hypothetical scenario, selection mosaics are likely to be congruent ($\delta_{S,H}\delta_{S,P} > 0$). There are, however, two caveats to this interpretation. First, the observed differences in the fitness consequences of infection must be environmental and not genetic. Second, other ecological factors, such as spatial variation in population densities, could also contribute to the selection mosaic. If these unmeasured factors contribute substantially to the structure of selection mosaics, the inferred sign of a selection mosaic could be incorrect.

Analysis of the simple model presented here has provided novel insight into the interplay between coevolution and local adaptation. Nevertheless, the results do rest on several assumptions that are likely to be violated in many natural populations. For instance, the model assumes that species interactions are mediated by a single diallelic diploid locus. This assumption constrains genetic diversity to levels well below those observed in some host-parasite interactions (e.g., Burdon et al. 2002; Frank 2002; Lively et al. 2004). In addition, the model has assumed that population sizes are effectively infinite, precluding potentially important effects of genetic drift (e.g., Burdon and Thrall 1999). These limitations of the model may partially explain why the average magnitude of local adaptation observed in simulations appears to be smaller than that detected in some empirical studies (e.g., Morand et al. 1996; Kaltz et al. 1999; Lively et al. 2004). This apparent discrepancy may also result, however, from a lack of statistical power to detect weak local adaptation or a bias toward selecting empirical systems characterized by particularly strong coevolutionary selection.

Taken together, the results verify key predictions of the geographic mosaic theory and raise alternative explanations for observed patterns of local adaptation in host-parasite systems. At the same time, however, the results demonstrate that coevolution in a geographic mosaic can lead to virtually any pattern of local adaptation or local maladaptation. Consequently, rigorous evaluation of the geographic mosaic theory will likely require empirical studies that focus on process rather than pattern.

Acknowledgments

I thank D. Browning, M. Dybdahl, S. Gandon, C. Goodnight, J. N. Thompson, and an anonymous reviewer for helpful comments. A special thanks to R. Gomulkiewicz and M. Whitlock for suggesting the separation of time scales approximation. This work was supported by National Science Foundation grant DEB-0343023.

Literature Cited

Agrawal, A., and C. M. Lively. 2002. Infection genetics: gene-for-gene versus matching-alleles models and all points in between. Evol. Ecol. Res. 4:79–90.

Ballabeni, P., and P. I. Ward. 1993. Local adaptation of the trematode *Diplostomum phoxini* to the European minnow *Phoxinus*, its second intermediate host. Funct. Ecol. 7:84–90.

Beerli, P., and J. Felsenstein. 2001. Maximum likelihood estimation of a migration matrix and effective population sizes in n subpopulations by using a coalescent approach. Proc. Natl. Acad. Sci. USA 98:4563–4568.

Burdon, J. J., and P. H. Thrall. 1999. Spatial and temporal patterns in coevolving plant and pathogen associations. Am. Nat. 153: S15–S33.

Burdon, J. J., P. H. Thrall, and G. J. Lawrence. 2002. Coevolutionary patterns in the *Linum marginale–Melampsora lini* association at a continental scale. Can. J. Bot. 80:288–296.

Dybdahl, M. F., and A. Storfer. 2003. Parasite local adaptation: Red Queen versus Suicide King. Trends Ecol. Evol. 18:523–530.

Endler, J. A. 1973. Gene flow and population differentiation. Science 179:243–250.

Fisher, R. A. 1950. Gene frequencies in a cline determined by selection and diffusion. Biometrics 6:353–361.

Flor, H. H. 1956. The complementary genetic systems in flax and flax rust. Adv. Genet. 8:29–54.

Frank, S. A. 2002. Immunology and the evolution of infectious disease. Princeton Univ. Press, Princeton, NJ.

Gandon, S. 1998. Local adaptation and host-parasite interactions. Trends Ecol. Evol. 13:214–216.

———. 2002. Local adaptation and the geometry of host-parasite coevolution. Ecol. Lett. 5:246–256.

Gandon, S., Y. Capowiez, Y. Dubois, Y. Michalakis, and I. Olivieri. 1996. Local adaptation and gene-for-gene coevolution in a metapopulation model. Proc. R. Soc. B 263:1003–1009.

Gomulkiewicz, R., J. N. Thompson, R. D. Holt, S. L. Nuismer, and M. E. Hochberg. 2000. Hot spots, cold spots, and the geographic mosaic theory of coevolution. Am. Nat. 156:156–174.

Haldane, J. B. S. 1948. The theory of a cline. J. Genet. 48:277–284.

Hey, J., and R. Nielsen. 2004. Multilocus methods for estimating population sizes, migration rates and divergence time, with applications to the divergence of *Drosophila pseudoobscura* and *D. persimilis*. Genetics 167:747–760.

Kaltz, O., and J. A. Shykoff. 1998. Local adaptation in host-parasite systems. Heredity 81:361–370.

Kaltz, O., S. Gandon, Y. Michalakis, and J. A. Shykoff. 1999. Local maladaptation in the anther-smut fungus *Microbotryum violaceum* to its host plant *Silene latifolia*: evidence from a cross-inoculation experiment. Evolution 53:395–407.

Kawecki, T. J., and D. Ebert. 2004. Conceptual issues in local adaptation. Ecol. Lett. 7:1225–1241.

Kraaijeveld, A. R., and H. C. J. Godfray. 2001. Is there local ad-

aptation in *Drosophila*-parasitoid interactions? Evol. Ecol. Res. 3:107–116.
Lively, C. M. 1999. The geographic mosaic of host-parasite coevolution: simulation models and evidence from a snail-trematode interaction. Am. Nat. 153S:S34–S47.
Lively, C. M., and M. F. Dybdahl. 2000. Parasite adaptation to locally common host genotypes. Nature 405:679–681.
Lively, C. M., M. F. Dybdahl, J. Jokela, E. E. Osnas, and L. F. Delph. 2004. Host sex and local adaptation by parasites in a snail-trematode interaction. Am. Nat. 164:S6–S18.
Morand, S., S. D. Manning, and M. E. J. Woolhouse. 1996. Parasite-host coevolution and geographic patterns of parasite infectivity and host susceptibility. Proc. R. Soc. B 263:119–128.
Nielsen, R., and J. Wakeley. 2001. Distinguishing migration from isolation: a Markov chain Monte Carlo approach. Genetics 158: 885–896.
Nuismer, S. L., and S. P. Otto. 2004. Host-parasite interactions and the evolution of ploidy. Proc. Natl. Acad. Sci. USA 101: 11036–11039.
Nuismer, S. L., J. N. Thompson, and R. Gomulkiewicz. 1999. Gene flow and geographically structured coevolution. Proc. R. Soc. B 266:605–609.
———. 2000. Coevolutionary clines across selection mosaics. Evolution 54:1102–1115.
———. 2003. Coevolution between hosts and parasites with partially overlapping geographic ranges. J. Evol. Biol. 16: 1337–1345.
Peters, A. D., and C. M. Lively. 1999. The Red Queen and fluctuating epistasis: a population genetic analysis of antagonistic coevolution. Am. Nat. 154:393–405.
Slatkin, M. 1973. Gene flow and selection in a cline. Genetics 75: 733–756.
Switkes, J. M., and M. E. Moody. 2001. Coevolutionary interactions between a haploid species and a diploid species. J. Math. Biol. 42:175–194.
Thompson, J. N. 1994. The coevolutionary process. Univ. of Chicago Press, Chicago.
———. 1999. Specific hypotheses on the geographic mosaic of coevolution. Am. Nat. 153:S1–S14.
———. 2005. The geographic mosaic of coevolution. Univ. of Chicago Press, Chicago.
Thompson, J. N., and J. J. Burdon. 1992. Gene-for-gene coevolution between plants and parasites. Nature 360:121–125.
Thompson, J. N., and B. M. Cunningham. 2002. Geographic structure and dynamics of coevolutionary selection. Nature 417: 735–738.
Thompson, J. N., S. L. Nuismer, and R. Gomulkiewicz. 2002. Coevolution and maladaptation. Integr. Comp. Biol. 42:381–387.
Thrall, P. H., and J. J. Burdon. 2003. Evolution of virulence in a plant host-pathogen metapopulation. Science 299:1735–1737.
Thrall, P. H., J. J. Burdon, and J. D. Bever. 2002. Local adaptation in the *Linum marginale–Melampsora lini* hostpathogen interaction. Evolution 56:1340–1351.
Tian, D., M. B. Traw, J. Q. Chen, M. Kreitman, and J. Bergelson. 2003. Fitness costs of R-gene-mediated resistance in *Arabidopsis thaliana*. Nature 423:74–77.

Corresponding Editor: C. Goodnight